Review

Recognizing potential of LiDAR for comprehensive measurement of sea spray flux for improving the prediction of marine icing in cold conditions - A review

Sushmit Dhar [a,*], Hassan Abbas Khawaja [b,c]

[a] *Department of Technology and Safety, UiT the Arctic University of Norway, Tromsø, Norway*
[b] *Department of Automation and Process Engineering, UiT the Arctic University of Norway, Tromsø, Norway*
[c] *Al Ghurair University, UAE*

ARTICLE INFO

ABSTRACT

Marine icing phenomenon depends on multiple variables like vessel characteristics and uncertain factors like environmental parameters, developing an accurate model for its forecasting, evaluation, and estimation is very challenging. Commonly, most severe ice accretion is caused due to sea spray. The past attempts to measure impinging sea spray flux were carried out on specific parts of the spray cloud, and most of the empirical spray-flux expressions presented only work in specific conditions. This necessitates further real-time and accurate field measurements of the entire impinging spray flux carried out in multiple scenarios in order to develop more practical correlation. High temporal and spatial resolution measurements and scanning ability of the LiDAR technique has proven to be useful in the agricultural domain for studying pesticide spray drift. This work reviews the past studies carried out using LiDAR technique for measuring the evolution of the pesticide spray cloud, asserting the potential of using a shipborne LiDAR for analysing sea spray in the study of marine icing phenomenon. The LiDAR system is capable to visualise the evolution of the sea spray drift with a high spatial and temporal resolution, which can enable comprehensive real-time measurement of spray flux for the entire sea spray cloud.

1. Introduction

Earlier industries have not shown much interest in the colder regions of our planet due to their focus on exploiting resources in easily accessible warmer regions. However, with the increase in competition in warmer regions, and the promising presence of natural resources, shorter transport distances and tourism opportunities, interest has grown to exploit these opportunities in marine cold climate regions. Shipping plays an integral part to utilise these opportunities as they are the preferred means for transportation, carrying out surveying operations, and also used as base stations. The growth of interest is evident from the significant surge in maritime traffic in the last few years. The total distance sailed by ships in the Arctic Polar Code area grew by 75% in 2019 compared to 2013 and predicted to increase substantially in the coming years (PAME, 2020).

Nevertheless, colder regions bring their challenges due to its remoteness and harsh weather. Icing is regarded as the most significant risk associated with colder regions; multiple vessels became disabled or sank after ice accretion leading to loss of life, damaging environment and property (Aksyutin, 1979; DeAngelis, 1974; Guest and Luke, 2005; Hay, 1956; Lundqvist and Udin, 1977; NTSB, 2018; Ryerson, 2013; Shekhtman, 1968; Shellard, 1974). Even after many years of research, advancement in analytical and numerical models, marine icing still possess a serious operational hazard for ships operating in cold climate regions (Cammaert, 2013). Hence it is crucial prior entering these regions to winterize a vessel effectively, which incorporates structural designs and techniques by adequate anti or de-icing, insulation and drainage system to decrease the adverse effects of icing and exposure to cold temperature (DNVGL, 2019). Past analysis of icing observations on ships depending on the geographical location indicated typically sea spray alone contributed 50–97%, spray along with atmospheric icing 41–1.4% and atmospheric icing alone 4-1% towards accumulation of marine icing over the vessels (Aksyutin, 1979; Brown and Roebber, 1985; Kato, 2012; Makkonen, 1984, 1984; 1984; Panov, 1976;

Shekhtman, 1968; Shellard, 1974; Zakrzewski, 1987). Sea spray ice accretion possess a substantial hazard to a vessel's seaworthiness as navigation, communication, safety, and other essential or critical equipment may become impaired, deck operation severely impacted and evacuation routes obstructed (Makkonen, 1984; Ryerson, 2013). The most imminent danger associated due to ice accretion for a vessel is the loss of stability which may ultimately lead to capsizing (Guest and Luke, 2005).

This paper focuses on the need for accurate real-time measurement of impinging sea spray, as the past researchers were only able to measure parts of a spray cloud and approximations were made based on the localised measured data. Hence there is a need for a different setup or a measuring technique which can measure the entire spray cloud in a comprehensive manner. The LiDAR (Light detection and ranging) technique has proven to be useful in the agricultural domain for studying pesticide spray drift measurement because of its measurement ability with high temporal and spatial resolution and scanning ability (Allard et al., 2007; Gregorio et al., 2016b; Richardson et al., 2017; Torrent et al., 2020). This shows the potential of using this technique in the field of marine icing for studying sea spray.

2. Sea spray icing and ship stability

The loss of stability is primarily threatening for smaller ships like fishing vessels (Orimolade et al., 2017), and almost 41% of ships entering the Arctic Polar Code area are fishing vessels (PAME, 2020).

Fishing vessels relatively have a lower freeboard and have a higher pitch angle and frequency; hence spray generation is more frequent and likely to cover the whole ship. The superstructure surface area is also large compared to its displacement, making them more exposed to sea spray. In the presence of low temperature, the spray freezes across the vessel and a comparatively lesser weight of accreted ice can destabilize and capsize the fishing vessel (Guest and Luke, 2005). When the vessel is propelling into the wind and waves, maximum ice accretion is on the forepart consequently trimming the vessel by head further intensifying incoming spray and green seas. Symmetric ice accretion (transverse) on the deck (Fig. 1), accommodation tops, and other higher parts shift the centre of gravity(G) upward and forward (Trim by head) along the centre line which reduces the metacentric height (GMt). This affects the dynamic performance by weakening righting lever (GZ) the ship's ability to upright when heeled by external forces, which is readily evident from the increase in the natural rolling period (also increase in heave and pitch period in a lesser extent) (Wold, 2014). Also, the Deck Edge Immersion angle is reduced due to reduced freeboard (extra weight of the ice), causing water ingression at a smaller angle of heel than initial. The vanishing angle of stability is reduced, which is an indicator of the overall range of stability (Chung, 1995). Due to ice accretion, the wind drag and sail area of the vessel increases, leading to an increase in the wind-induced heeling moment. Gradually with the increase in ice load, the metacentric height keeps decreasing to negative eventually unable to upright leading to its capsizing. Depending on the relative direction of wind and waves, an asymmetrical sea spray ice accretion
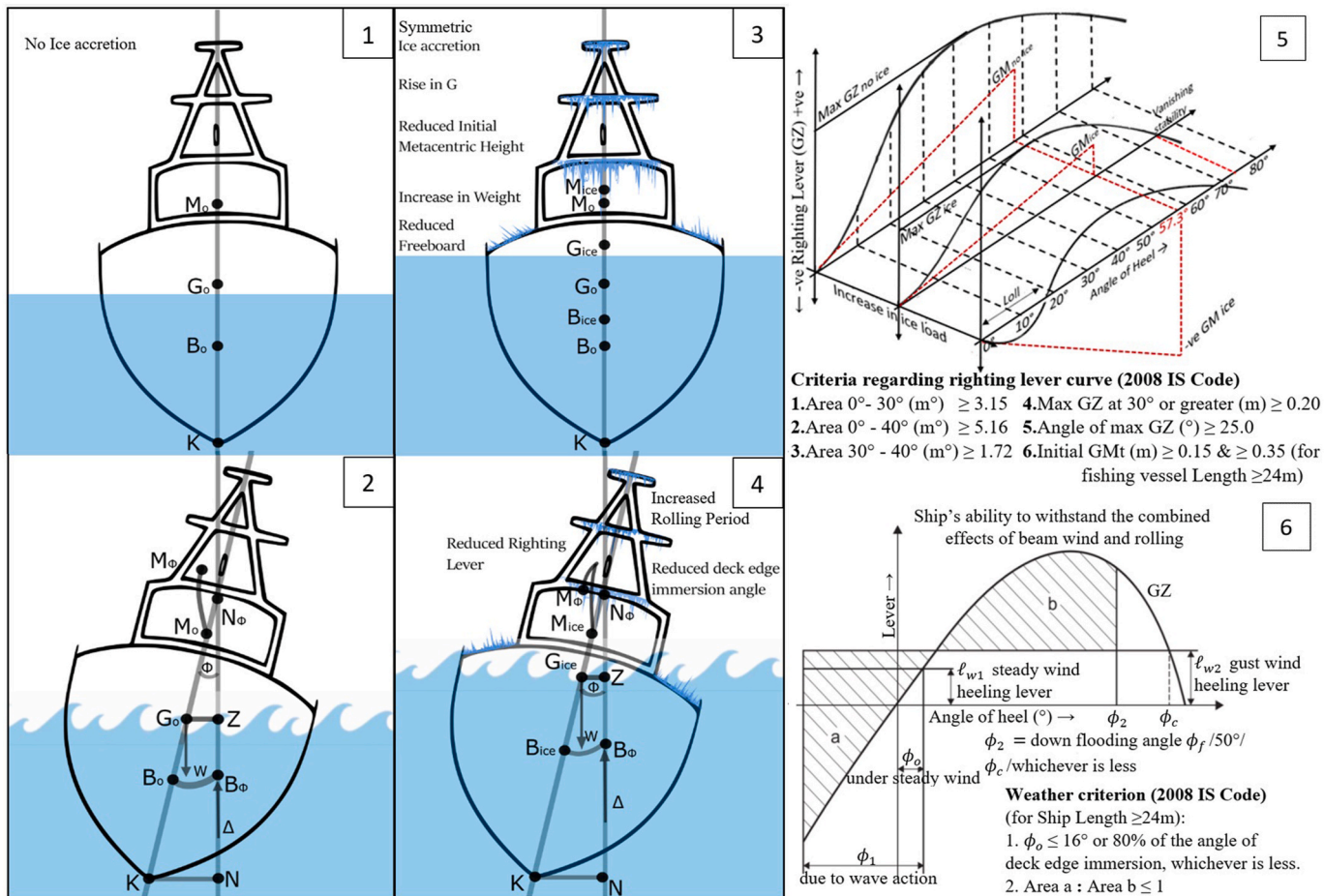

Criteria regarding righting lever curve (2008 IS Code)
1. Area 0°- 30° (m°) ≥ 3.15   4. Max GZ at 30° or greater (m) ≥ 0.20
2. Area 0° - 40° (m°) ≥ 5.16   5. Angle of max GZ (°) ≥ 25.0
3. Area 30° - 40° (m°) ≥ 1.72   6. Initial GMt (m) ≥ 0.15 & ≥ 0.35 (for fishing vessel Length ≥24m)

Weather criterion (2008 IS Code)
(for Ship Length ≥24m):
1. ϕ_o ≤ 16° or 80% of the angle of deck edge immersion, whichever is less.
2. Area a : Area b ≤ 1

ϕ_2 = down flooding angle ϕ_f /50°/ ϕ_c /whichever is less

Fig. 1. Vessel with no ice accretion in calm weather (1) Vessel able to upright instantly when heeled (2) Vessel with reduced stability due to ice accretion (3) Vessel's righting ability reduced when heeled (4) Righting Lever curve of a vessel getting unstable with the gradual increase in ice load (5) 2008 IS Code- Severe wind and rolling criterion (6) Abbreviations: G_o- Centre of Gravity (No ice accretion), M_o- Metacentre (No ice accretion), B_o- Centre of Buoyancy (No ice accretion), K - Keel, ϕ - Angle of heel, B_ϕ- Centre of Buoyancy (after heel), N_ϕ- False Metacentre, M_ϕ - Actual metacentre when heel, GZ - Righting Lever, B_{ice}- Centre of Buoyancy (ice accretion), M_{ice}- Metacentre (ice accretion).

can cause the centre of gravity to shift upward and away from centre line causing the vessel to list, further increasing its tendency to capsize (Chung, 1995). The International Code on Intact Stability (2008 IS Code) (IMO, 2020) and the Polar Code (IMO, 2016) includes allowance for ice accretion ("30 kg/m^2 on exposed weather decks and gangways and 7.5 kg/m^2 for the projected lateral area of each side of the ship above the water plane"), which should be incorporated in the stability calculation for ships at risk of icing, ensuring its adequate stability.

3. Sea spray ice accretion

Typically sea spray ice accretion can be divided into three parts:

3.1. Sea spray cloud generation

The high energy impact of wave and ship results in the formation of water sheet along its hull, as the water sheet upsurges above the water level, air enters and the sheet break into drops, and gradually forms a cloud of droplets (Dehghani et al., 2016a). These generated droplets reach variable heights and velocities depending on the kinetic energy of the collision and diameters ranging from 10 μm to 3 mm close to the bow (Bodaghkhani et al., 2016; Rashid et al., 2016; Ryerson, 2013; Zakrzewski, 1986). The wave generated spray is a significant source of water flux which is the main contributor for marine ice accretion and often formed close to the vessel's bow depending on relative motion and likely have a short and periodical frequency (Hansen, 2012). Sea spray may also be generated by strong wind shearing droplets off wave crest and by bubbles bursting in breaking waves creating atomized droplets ranging ≤1 μm to ≥25 μm (Fuentes et al., 2010). Wind-generated droplets usually have a relatively much lesser but continuous contribution to the icing phenomena (Dehghani-Sanij et al., 2015).

3.2. Sea spray cloud drift and impinging upon the ship's structure

The sea spray cloud generated is then carried by the airflow across the vessel until finally impacting components or structures on the vessel. The droplets in the cloud of different initial velocities, sizes and shapes are influenced differently by wind and gravitational force, and their paths and trajectories are specified through drag force, body forces and added mass force acting on it (Dehghani et al., 2016a; Kulyakhtin and Tsarau, 2014; Makkonen, 2000). The wind carries the small droplets with their velocities nearly become similar to the velocity of the wind, but the large droplets being affected more by the gravitational force shortly drops on the deck or back to the sea. The larger and smaller droplets are not able to reach the highest elevation of the spray, while the trajectory of the medium-sized droplets makes it (Dehghani et al., 2016b). The characteristics of the spray droplets may change anytime along their path, may reduce in size due to evaporation or aerodynamic breakup, or increase when combining with another droplet (Lozowski et al., 2000). LWC(Liquid water content) which is the total mass of the water droplets in a unit volume of dry air, is an important parameter of incoming spray flux along with velocity and distribution of the droplets for icing calculation (Dehghani-Sanij et al., 2017a).

The heat transfer, vaporization and temperature change during the drift of the droplets are determined by the characteristics of the droplet like velocity and size (Dehghani-Sanij et al., 2017a, 2017b; Kulyakhtin and Tsarau, 2014; Sultana et al., 2018). The droplets undergo convective, evaporative and radiative heat transfer, cooling the droplets within the airflow during the drift and eventually supercooled. When the supercooled droplets impact and splash on the substrate, creates ice followed by running off brine water due to gravity and tensile stresses from the air forms a layer or film, and at the same time losing heat via conduction, convection, and radiation (Kulyakhtin and Tsarau, 2014; Ryerson, 2013). The state of freezing droplets is reliant on properties like its size, salt content and also the thermal behaviour of the substrate

(Saha et al., 2016).

3.3. Wet growth of ice from the brine water film

The majority of the brine water film drains off from the ice surface entrapping a small amount leading to the growth of ice or Wet growth (Makkonen, 1987). The rate at which the brine film freezes and the consequent wet growth, is dependent on the incoming water flux transported at different areas on the vessel, and the rates at which latent and sensible heat extracted from these areas (Ryerson, 1995). The sea salt precipitates with growth in ice thickness forming pure ice and pockets of brine (Rashid et al., 2016). The primary heat fluxes at the air-water interface contributing to the freezing of sea spray impinging at the accreted ice surface are - convective or sensible heat flux from the air (Q_c), evaporative or latent heat flux from the air(Q_e), heating or cooling from impinging spray(Q_d) and heating or cooling from radiation (Q_r) (Kulyakhtin and Tsarau, 2014; Samuelsen et al., 2017).

Latent heat released during freezing $\left(Q_f\right) = Q_c + Q_e + Q_d + Q_r$　　　equation 1

4. Need for real-time data

We had discussed how the spray cloud generated from wave and wind spray is the primary cause of icing on the vessel. Dehghani et al., 2016b describes the process of spray cloud generation, and its movement into several sub-stages including wave impact, water sheet breakup, droplet breakup, spray cloud generation, its acceleration and deceleration and spray cloud fall and finally impingement. However, the physical behaviours of these stages are still inadequately understood. Characteristics of spray clouds such as its duration and movement in the airflow determining incoming water flux are an essential aspect to model the marine icing phenomenon (Kulyakhtin and Tsarau, 2014). The accurate prediction of marine icing and the quantity of ice accretion on the vessel structure is challenging mainly because of the variable quantity of incoming flux at different parts of the vessel which is affected by multiple parameters (Fig. 2) at the same time. Past studies (Dehghani-Sanij et al., 2015; Horjen, 2015, 2013; Kulyakhtin and Tsarau, 2014; Lozowski et al., 2000; Shipilova et al., 2012) did not consider the distribution and variation of droplet size and velocity in a spray cloud for their icing models (Dehghani et al., 2016b). The empirical models and nomograms for predicting icing severity (Comiskey et al., 1984; Itagaki, 1977; Kachurin et al., 1974; Makkonen, 1984; Mertins, 1968; Overland et al., 1986; Overland, 1990; Stallabrass, 1980; Sawada, 1962; Wise and Comiskey, 1980) were mostly built on data obtained from small to medium sized vessels, and based on input parameters of atmospheric conditions, which makes their applications confined to particular regions (Sultana et al., 2018). Also, by investigating present analytical models, it was found in order to make them more effective, further research and precise measurements are required for calculating the thermo-physical properties and heat transfer phenomena (Sultana et al., 2018). The efficiency of the predicted icing rates even from the present advanced models of sea-spray icing even with increased accuracy of the numerical prediction models, depends on the correctness to which the complex and uncertain quantities like spray flux, turbulent heat transfer, and the freezing temperature are predicted (Samuelsen and Graversen, 2019).

The significant difficulties in modelling spray cloud generation, propagation and finally impingement are:

1. The wave, wind and environmental parameters are highly dynamic, irregular, interdependent and may have varied scenarios in the cold regions.
2. The spray flux, its liquid content, the spray duration and frequency depend on the ship design, its speed over water and heading with respect to the wind and waves and its dynamic behaviour. Ships of
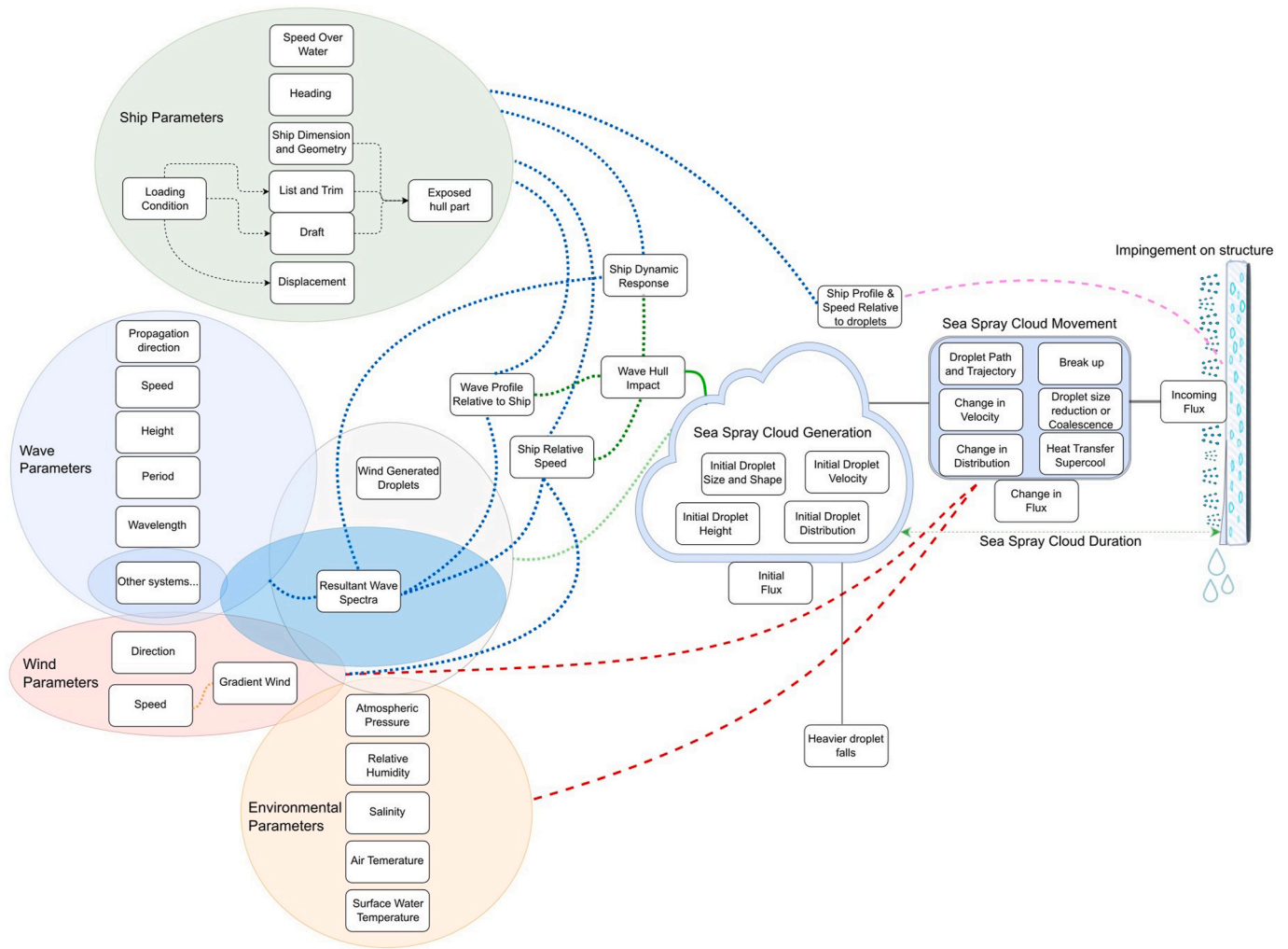
Fig. 2. Showing the complexity and interdependencies in the process of sea spray cloud formation, propagation and impingement.

different geometry, dimension and loading condition interact differently with sea conditions.

3. There is a lack of understanding in the behaviour of the droplet during its propagation within the turbulent flow around different types of ship's structure and the near-field biases caused by airflow alterations over the vessel. This ultimately decides the distribution and quantity of incoming water flux at different locations on the vessel, hence questions the reliability and versatility for predicting marine icing from the CFD models, which is also restricted by

uncertainties like spray generation method. Moreover, all these models are lacking validation against field observations (Mintu et al., 2016).

This necessitates direct measurements to gather real-time data of the concentration or spatial distribution of the entire impinging spray to remove errors from each step, in order to develop more practical and functional equations. The formulae used to calculate LWC in a spray cloud, only presents an estimation (Dehghani-Sanij et al., 2017a). The different empirical correlations (Table 1.) are obtained from observation for a distinct set of conditions and do not take into account different

Table 1
LWC empirical correlations based on different conditions of spray cloud generation (Rashid et al., 2016).

Reference	LWC correlation	Correlation variables
Borisenkov et al. (1975); Samuelsen et al. (2015); Zakrzewski (1987)	$w = w_o H_s \nu_r^2 e^{-0.55h}$	w is LWC of spray cloud (kg/m^3)
Borisenkov et al. (1975); Roebber and Mitten (1987)	$w = w_o' H_s^{2.5} e^{-0.55h}$	w' is averaged LWC of spray cloud (kg/m^3)
Forest et al. (2005)	$w = 1.35 H_s^2 e^{-0.53z'}$	H_s is significant wave height (m)
Stallabrass (1980)	$w' = 1.7 \times 10^{-4} H_s$	z is spray cloud elevation above mean sea level (m)
Kachurin et al. (1974)	$w' = 10^{-3} H_s$	h is elevation above the vessel deck (m)
Horjen and Vefsnmo (1984)	$w = 0.1 H_s e^{(H_s - 2z)}$	H_{rms} root mean square wave height (m)
Brown and Roebber (1985); Forest et al. (2005)	$w = 4.6 e^{-\left(\frac{2z}{H_{rms}}\right)^2}$	z' is spray cloud elevation above wave wash zone (m)
		ν_r is ship speed relative to incoming wave (m/s)
		$w_o = 6.36 \times 10^{-5}$ (empirical constant)
		$w_o' = 1.3715 \times 10^{-3}$ (empirical constant)

vessel parameters; so, they may provide incorrect results if generalised (Rashid et al., 2016; WMO, 1994; Bodaghkhani et al., 2016). Dehghani et al. (2016b) reviewing past sea spray icing models, mention that the lack of recording the distribution of size and velocity in a spray cloud led the researchers to use mono-size and mono-velocity models. There is a lack of empirical observations; consequently, the analytical and numerical formulations are based only on a few actual field observations and not comprehensive data (Dehghani-Sanij et al., 2017a). Hence, there is a need for more accurate field measurement, considering more parameters and scenarios.

5. Past sea spray field measurements

Some researchers carried out measurements in the past, attempting to measure real-time incoming sea spray on vessels to formulate or validate incoming spray flux or liquid water content correlation and model its distribution to estimate sea spray icing accurately. Tabata et al. (1963) reported field measurements on a few Japanese ships, during which both ice accretion rate and the sea spray intensity were measured (Zakrzewski, 1986). Specially designed icing gauges consisting of a rod suspended in a weight gauge were placed over the ship to measure the icing rate and entrap the sea spray (Lundqvist and Udin, 1977). Later, Tabata (1969) measured the spray amount and distribution on deck aboard a 350-metric ton patrol vessel, with his instrument consisting of water absorption sheet (toilet tissue) in circular cylinder distributed across the forecastle, which was replaced every 5–6 min interval. Then measured the added mass from spray events, fluxes fluctuated from 0.06 to 0.98 kg/m^2/h depending upon the cylinder's location on the bow area, and relative wind speed and wave direction (Ryerson, 1995). Brown and Roebber (1985) used the above data sets to present a relation, of the change of time-averaged spray flux as a function of the ship's speed and heading (Zakrzewski, 1986). Ono (1964) measured ice growth rates and the sea spray intensity on patrol boats, from the accreted amount of spray on an icing rod and collecting the excess runoff brine in a calibrated jar (Ozeki et al., 2016). Itagaki (1984) used this data as a function of air temperature and wind speed to estimate the ice accumulation rate on stationary structures. Sharapov (1971) study provided a data set from a medium fishing vessel (MFV) recording the spraying zone extent for wind speed from 5 to 11 Beaufort. Later, Zakrzewski et al. (1988) used this data for validating the model performance for his correlation for calculating the highest extent spray droplets from wave hull interaction, which was based on field icing data from Kuzniecov et al. (1971). Gashin's study mentioned in Borisenkov & Panov (1972) provided the first direct measurement data for bow-generated spray characteristics, from the analysis conducted on a MFV of 35 m long Soviet fishing trawler. In his data, the spray droplet diameters ranged between 1000 μm and 3500 μm with a mean of 2400 μm, but his measurement methods, environmental and sea conditions during his field trial and variations of his result with different vessel size are not known (Ryerson, 1995). Kachurin et al. (1974) formulated the first LWC correlation as a function of wave height only based on measurement from a MFV, but stated no information about the measurement technique. Borisenkov et al. (1975) published data of spray cloud field measurement made on a MFV in the Sea of Japan, reported ship and environmental parameters though information about droplet size and velocity distribution were are not stated. The data was also used for producing empirical LWC formulation and succeedingly used by Zakrzewski (1986) and Brown and Roebber (1985) for extending the formulation, and later showed by Samuelsen et al. (2015) the variation in the empirical constant value varies from the previous study. Method of directly measuring spray flux was carried out in the 1980s on an artificial island (Tarsiut Island) to develop the RIGICE model, the spray data collected from measuring the water level at hourly intervals in 45-gallon drums (Muzik and Kirby, 1992). As a part of the study program "Offshore icing" (Horjen et al., 1986; Jørgensen et al., 1986) measurement of spray flux was carried out on supply vessels, stand-by

boats and offshore structures for calibrating the Norwegian marine icing model ICEMOD (Horjen, 1990), the data is also utilized by the later developed icing models MARICE and NuMIS. Spray measurements were carried out with absorption panels consisting of absorbent paper (paper diapers) and bent pipes collecting the impinging spray into a graduated container (Teigen et al., 2019), but no information related to spray droplets were provided (Bodaghkhani et al., 2016). Ryerson (1995) was the first to carry out the real-time measurement of sea spray on a larger ship (CGC Midgett 115 m length). His experimental setup consisted of vertical and horizontal oriented funnel-shaped spray collectors, ultrasonic range-finding ice detectors, video recording systems and stroboscopic droplet camera. Characteristics of the spray cloud generation frequency, duration, height and distribution size were recorded. Also, parameters such as sea and environmental conditions, ship position, speed, and heading, were logged for every hour. The spray flux was measured at six different locations, but the result presented was only for one location. The reported incoming droplet size varied from 14 to 7700 μm, and median of 234 μm, the mean droplet concentration about 4×10^5 droplets/m^3, the average cloud droplet concentration of 1.05×10^7 droplets/m^3 and average spray event duration 2.37 s was recorded (Dehghani et al., 2016b). He also attempted to form the LWC correlation, but the comparison among his measurements and past LWC correlations were not satisfying. Though his result provided crucial data set, however, it was based on specimens from the spray cloud and not based on accounting for the entire distribution data set of the entire spray cloud, and also, the model did not include the droplet velocity data (Bodaghkhani et al., 2016; Dehghani et al., 2016a). Jones and Andreas (2013) collected sea spray at Mt. Desert rock lighthouse catwalk at 20 m above sea level, to inspect spray generated over the ocean instead from wave and shore impact and was observed under microscopic slides. This project's long-term goal is to estimate the sea spray concentration across the open ocean and sea spray icing on offshore constructions. Ozeki and Sagawa (2013) modified a snow particle counter into seawater particle counter (SPC), it consisted superluminescent diode light as a parallel ray measuring light attenuation by particles passing through the sensing area (25 mm wide, 3 mm high, and 0.5 mm deep). The SPC was able to measure the droplet size distribution impinging the sensing area every second and was placed on the upper deck of an ice breaker, and the measuring range was set from 100 to 1000 μm in diameter. By using the result, the flux distribution and the transport rate could be approximated as a function of particle size. Johansen et al. (2015) proposed a study of using a high-speed camera for imaging sea spray and using image analysis (Hough Transform) for measuring the Sea Spray Flux. However the study could not be deployed for field test because other than the setup being too expensive, most critically it required very sensitive lightning setup, which is very difficult to control in the harsh marine climate. Ozeki et al. (2016) modified a marine rain gauge to measure seawater spray in large ships, and found a correlation in measurement with their previously developed seawater particle counter (SPC). Measurement of seawater spray was performed on the compass deck and the bow deck of an icebreaker.

Teigen et al. (2019) describes the real-time autonomous measurement system designed by modifying a tipping bucket to collect sea spray to measure and record continuous flux on offshore facilities as part of the joint industry project RigSpray. The system (Fig. 3.) consists of flux meters consisting of a collector plate (dimensions 0.5 m × 0.5 m) funnelling the impinging spray to a tipping bucket via a small hose. The tipping bucket's water level is continuously measured with a wireless gauge pressure, and the water empties automatically after reaching a certain level. The system also includes a video recording system and can transmit the data wirelessly and has been in operation on the ship shaped FPSO unit "Norne" in the Norwegian Sea. The project provides spray measurements data along with corresponding vessel motion and environmental dataset important for calibrating spray models on large ship-shaped offshore structures (The RigSpray icing model, Bøckmann et al., 2019).
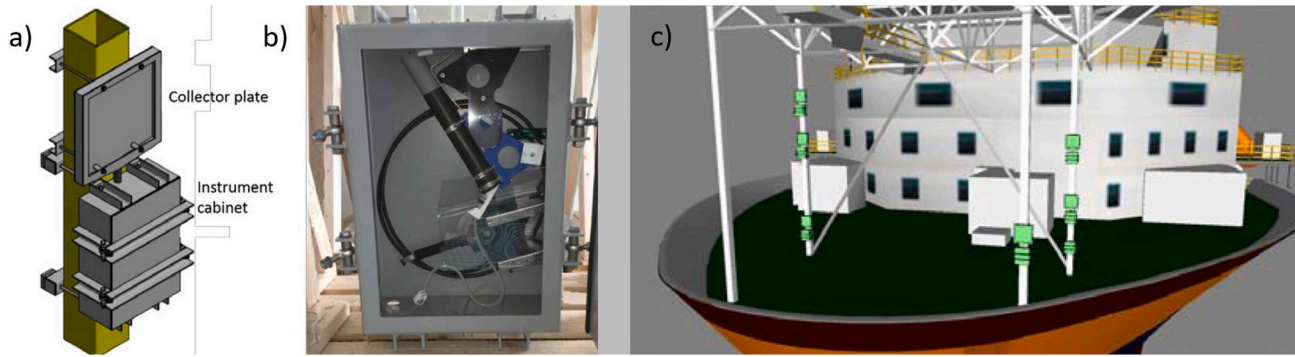
Fig. 3. (a) Fluxmeter Design (b) Instrument cabinet with the tipping bucket (c) Mounting positions of the six fluxmeters in the bow of the Norne FPSO (Teigen et al., 2019).

The measurement techniques and data collection and analysing procedures have improved over time and have proven to be helpful because of its simplicity and robustness in the harsh climates. However, the past studies were only able to measure samples of spray flux from some specific parts of a spray cloud and approximations were made on the basis of the localised measured data. So, for other conditions, the droplet size and concentration need to be assessed for the entire spray cloud from the approximated proposed distribution. Also, the prevailing micrometeorological conditions substantially affect the results during the field trials varyingly at different locations on the ship. Hence, they fail to provide a factual comprehensive time-resolved distribution data set for the entire spray cloud. Information the past studies could not provide about the entire impinging spray cloud such as its complete droplets distribution, velocity, and concentration which is inherent for the formulation of accurate correlation of spray flux, vertical distribution, and the spray cloud's maximum height. Therefore, it is necessary to adopt different setups or measuring techniques which can carry out real-time monitoring in spatial and temporal resolution to measure incoming sea spray flux for the complete spray cloud with higher efficiency and accuracy.

LiDAR (Light detection and ranging also known as laser radar) is an optical sensing technique that has the potential to breaks through the shortcomings mentioned above, as it is possible to use this technology for carrying out real-time active measurement of entire spray cloud with high temporal and spatial resolution.

6. LiDAR

LiDAR is a long-existing active range-resolving optical measurement technique and commonly used for remote sensing and analysing of aerosols and clouds in atmospheric studies and presently has broad application throughout almost every field (Gregorio López, 2012;

Hulburt, 1937; McManamon, 2019).

LiDAR is a popular choice in atmospheric studies as it can provide high temporal and distance resolution, due to the substantial interaction between the emitted electromagnetic radiation at optical wavelengths (ranging from ultraviolet to near-infrared) and aerosols or molecular components in the atmosphere (Measures, 1992). Elastic LiDAR technique (Fig. 4.) is the most commonly used technique, operating by the emitting pulsed lasers and detecting backscattered radiation at the same wavelength, and the delay in receiving signal computes (time of flight) the distance (equation 3). Pulsed elastic LiDARs provide a range-resolved intensity profile of the received signal. Following the principle of simple scattering, this intensity profile follows the LiDAR equation, expressed as received power component (equation 2) (Collis and Russell, 1976; Gregorio López, 2012). Other LiDAR techniques such as Raman LiDAR (inelastic), Differential Absorption LiDAR (DIAL) and doppler LiDAR are also used in atmospheric studies.

| Receiver Power equation 2	$P(\lambda, R)$ Receiver Power (W)
$$P\left(\lambda, R\right) = P_o\left(\frac{c\tau_l}{2}\right)\beta(\lambda,R)\frac{A_r}{R^2}exp[- 2\int_0^R \alpha(\lambda,r)dr]\xi(\lambda)\xi(R)$$	λ wave length (nm) R distance (m) P_o Peak Transmitted Power(W) c speed of light (m/s) τ_l emitted laser pulse duration (s) τ_d temporal detection window (s) $\beta(\lambda,R)$ volumetric backscattering coefficient (/m/sr) A_r Effective area of the receiver telescope (m^2)
Spatial Resolution equation 3 $$\Delta R = \frac{c(\tau_l + \tau_d)}{2} \approx \frac{c\tau_d}{2}, \tau_{l<<\tau_d}$$	$\alpha(\lambda, r)$ volume extinction coefficient (/m) $\xi(\lambda)$ Spectral transmissivity factor of the emission-reception optical system $\xi(R)$ Overlap factor between the emitted laser beam and the receiver field view
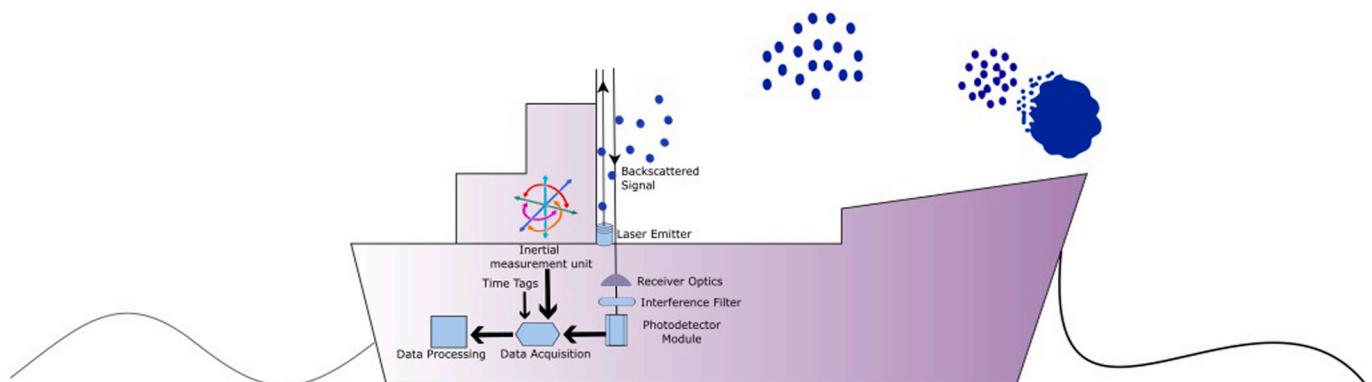
Fig. 4. Conceptual LiDAR set up for analysing sea spray.

7. Past spray drift studies using LiDAR technology

Due to the high temporal and spatial resolution and latterly scanning ability, LiDAR systems had been fairly utilized as a method for monitoring pesticide spray drift and particulate matters in the agricultural application. Some of the promising studies used for monitoring spray drift are mentioned which shows its potential to be used in the field of marine icing for analysing sea spray cloud.

The first research carried out by the U.S. Forest Service, Stanford Research Institute group in 1966–1967, investigating the use of LiDAR to monitor the dispersal of insecticide spray in the forests of Idaho. Air motions were observed by tracking spray and smoke clouds and also displayed how turbulent, and other diffusive processes can be analysed (Collis, 1968). Atmospheric Environment Service (AES) of Canada constructed an elastic backscatter LiDAR system (ARAL) capable of fast attainment to analyse spray geometry and deposition of pesticides from an aerial application by scanning the cross-section of the spray (Hoff et al., 1989). Later ARAL was used by Mickle (1994), 1996 to analyse the dynamics of the pesticide spray when aerially released. LiDAR technology also had been used and proven to be an ideal tool to validate theoretical spray-movement models and was able to expose the discrepancies in the models (Mickle, 1999; Stoughton et al., 1997; Tsai, 2007). Another elastic backscatter LiDAR was used to monitor aerially applied biological pesticide spray to support the hypothesis that a widespread dispersal of a small pesticide quantity is unavoidable, even if the operation is adequately handled (Miller and Stoughton, 2000). Miller et al. (2003) used LiDAR ground spray measurements to create 3D images of the spray drift cloud above an orange farm. Hiscox et al. (2006) introduced a methodology to estimate the spray cloud absolute concentration obtained from the LiDAR return signal. From the spray application rate and the initial droplet size distribution, theoretical models of evaporation and deposition were used to simulate droplet quantity's temporal evolution, which remains in the air from aerial spray application. They detected a satisfying correlation in the concentrations estimated from the derived model and the LiDAR return. Institute National d'Optique (INO), Canada specially developed an eye-safe close range (<100 m) LiDAR for the purpose of monitoring pesticide spray drift (Allard et al., 2007; Cantin et al., 2007). Prior this most studies used LiDAR systems whose design was architected for far range atmospheric studies.

The INO LiDAR prototype was tested to validate its performance in the applications of pesticide and dust cloud monitoring. The digitized waveform (Fig. 5.) of the backscattered signals demonstrated that the equipment was able to monitor low signal levels from the water spray drifting cloud (tested with water instead of real pesticide) as well as high signal levels from solid targets (like dust). The result also showed the ability of LiDAR to present important measurement data regarding the relative concentration of airborne aerosols of diverse nature, also at a shorter range (Allard et al., 2007). Khot et al. (2011) describes the methodology used to report the application of calibrated LiDAR to quantify spray distribution across space and time. The results exhibited a linear relationship ($R^2 \approx 0.77$) between LiDAR backscatter signal of the spray plume and passive spray collection on samplers. Miller et al. (2012) applied LiDAR to analyse spray drift from near-ground aerosol fogs in several stability conditions concluding that spray coverage is more extensive under strong wind. A commercial ultraviolet LiDAR system (ALS 300, Leosphere, Orsay, France) was used to monitor spray drift (Fig. 6.) for comparing with the measurements obtained from the passive collectors which is conventionally used for measuring pesticide spray drift. The result of the analysis showed a strong linear correlation ($R^2 \approx 0.90$) proving LiDAR to be a better alternative for monitoring pesticide spray drift with lesser time and resources (Gregorio et al., 2014).

An eye-safe LiDAR system was explicitly designed for the purpose of spray drift monitoring (Gregorio et al., 2015), with a scanning ability via pan and tilt unit up to 25°/s and 12°/s in azimuth and elevation (Gregorio et al., 2016b). The instrument has a laser emitter (Er-glass laser) of 1534 nm wavelength, emitting pulses of 3 mJ energy and 6ns duration. A telescope with 80 mm aperture captures the backscattered light, and it is directed on the photodetector surface of an avalanche photodiode (APD) module which converts the received light to electrical signal (Gregorio et al., 2016b).

The temporal and spatial resolution and scanning capability of the LiDAR equipment were tested to observe real time behaviour of the drift cloud (Fig. 7 and 8.) under different spray conditions and the author claimed LiDAR to be an appropriate method to carry out drift measurement with much lesser time, cost and labour compared to using passive collectors (Gregorio et al., 2016a, 2016b).

The past spray studies carried out in the agricultural domain provide evidence for LiDAR's temporal and spatial resolution capabilities to monitor the entire spray cloud's real-time behaviour, which the past sea spray studies failed to provide. Moreover, the LiDAR system enables evaluation of the spray drift speed, its concentration and evolution with time and ultimately providing a broader view. These results are encouraging to propose this technique, which can be valuable in the field of marine icing due to the similarities of pesticide spray with sea spray for studying the complex sea spray behaviour under different circumstances.
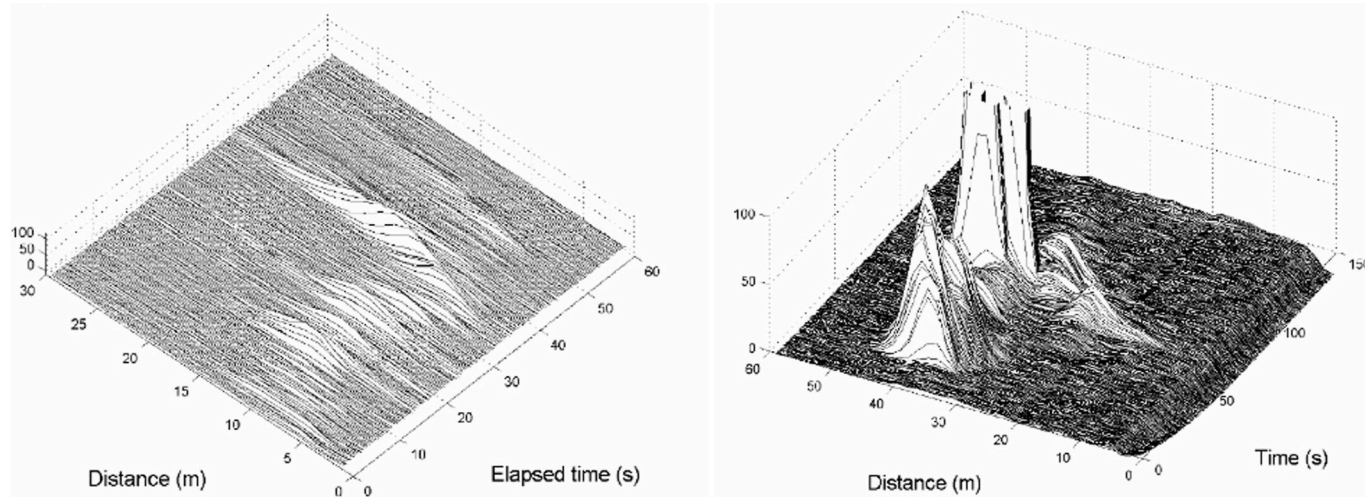

Fig. 5. Showing the time and distance evolution of the backscattered signals from the spray clouds of water droplets (left) and from the dust clouds (right) (Allard et al., 2007).
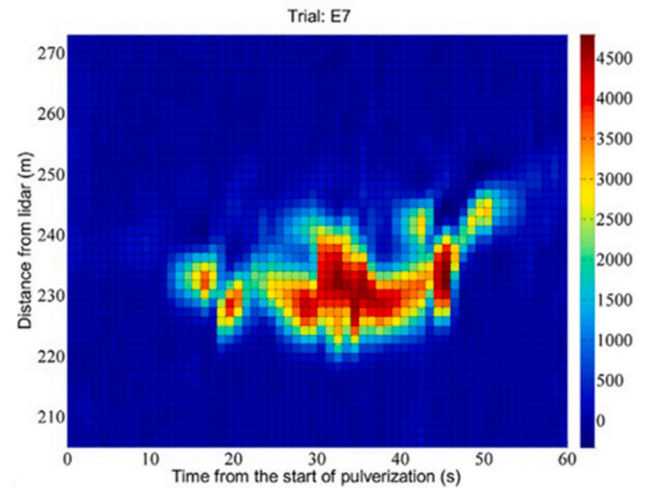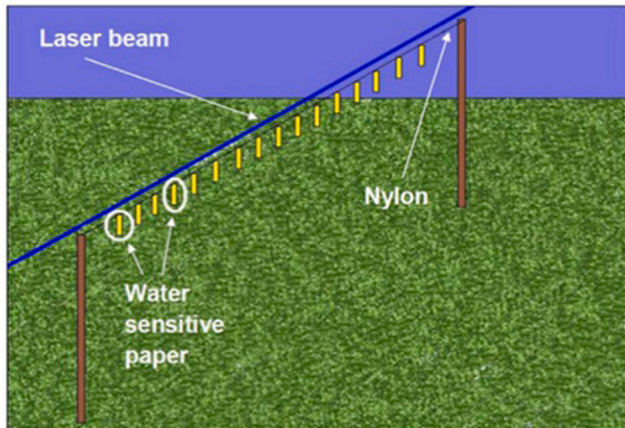
Fig. 6. Showing experimental setup (left) and Range-corrected background-subtracted LiDAR signal (arbitrary units) with a range resolution of 1.5 m and temporal resolution of 1s (right) (Gregorio et al., 2014).
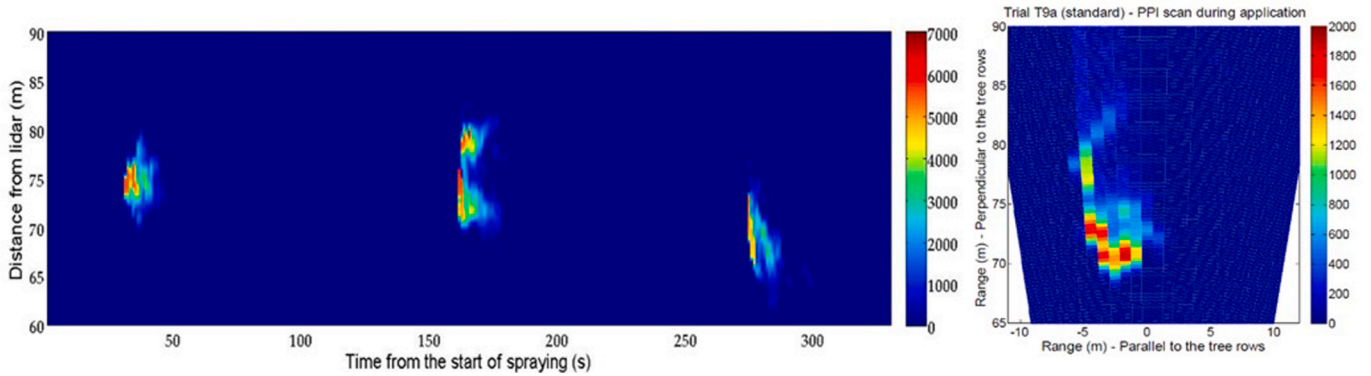

Fig. 7. spray flux over the canopy with temporal (1 s) and spatial (2.4 m) resolution (left) and 2D scans of the spray flux over the canopy, both in azimuth and elevation (right) (Gregorio et al., 2016a).
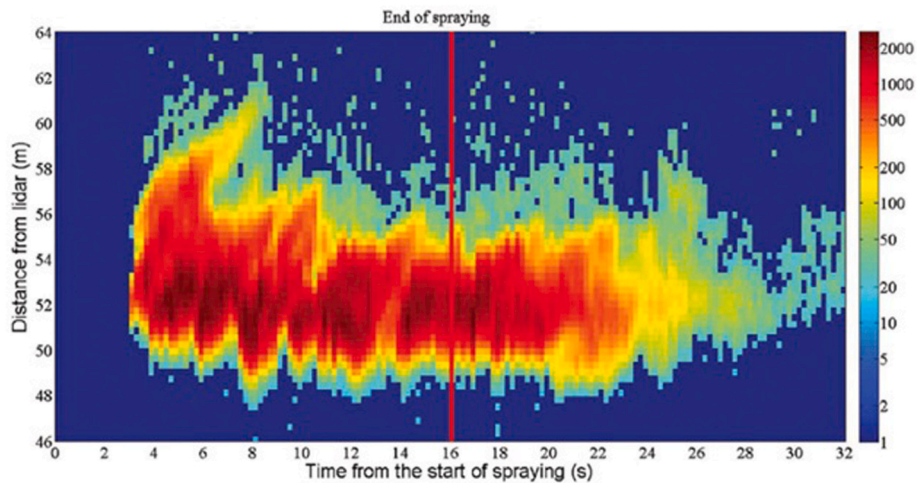

Fig. 8. Range time intensity plot of spray drift with high temporal (200 ms) resolution (Gregorio et al., 2016b).

8. Shipborne LiDAR for sea spray measurement

Application of a LiDAR system suitable for shipborne use for the analysis of sea spray will encounter certain technical challenges that need to be incorporated during the selection of the equipment or during its design phase. The ability for near-range measurement with a high spatial and temporal resolution is essential; besides the equipment being compact, have low power consumption, eye-safe and able to withstand the harsh marine environment is also important.

8.1. Near-range measurement using LiDAR

Conventional LiDAR systems were mainly designed for analysing and measuring tropospheric atmospheres. Hence, they transmitted high-power pulsed laser (used Ruby, YAG, and YLF lasers till the mid-90s) and had large aperture receiver telescopes in order to carry out far range measurements (Gregorio López, 2012). The system used were complicated, heavy, high power consumption, requiring highly skilled operators and costly (Ansmann et al., 1997; Fiocco and Smullin, 1963; Sassen, 1975). Technological improvements in the last years concerning efficient low-energy and high-PRF lasers and affordable photodetectors in the eye-safe region, let to rise in its application in near range observations such as aerosol-flow imaging, monitoring industrial emission, gas leak detection, etc.(Edner et al., 1995; Fukuchi and Shiina, 2012; Miya et al., 2009; Song et al., 2020). Micro Pulse Lidars (MPL) (Spinhirne, 1993, 1994) and modern commercial ceilometers (Madonna et al., 2014; Muenkel et al., 2004; Song et al., 2017) paved the way for economical, compact and convenient LiDAR systems. Development in laser technology with Laser diodes (LD) and Diode-Pumped Solid-state (DPSS) further made LiDAR more compact and have found a widespread application (Kong et al., 2018; S. Lolli et al., 2011). A LiDAR deployed on ships for sea spray measurement should have the capability for short-range measurement with a comparatively smaller field of view, along with being compact with lesser power consumption and have to be reliable in the marine environment. With state-of-the-art advancements, Light Emitting Diode (LED)-based light source has become popular for short-range measurements. Shiina and Koyama (2010a) from Chiba University, Japan developed compact, lightweight mini LiDAR with a Light Emitting Diode (LED)-based light source for near-range measurements (around 0–100 m), since then it had been utilized in widespread short-range application from MARS rover to atmospheric study among others (Koyama and Shiina, 2011; Ong et al., 2018; Shiina, 2010b, 2013, 2019a, 2019b, 2020; Shiina et al, 2015, 2016). The LED lamp module has a larger divergence compared to laser beams, does not require a heat sink or fan and claims to be cheaper, provide a wide range of wavelength choice, lesser power consumption, resilient against static electricity and has extended duration of use with consistent intensity (Shiina, 2019a), hence has a potential for onboard use for analysing sea spray.

8.2. Motion compensation

A LiDAR mounted on a ship for sea spray analysis is going to experience six-degree translation and rotational motion induced by the floating vessel due to action of wind and waves, which will introduce distortions in the LiDAR measurement. This motion needs to be compensated for getting an efficient assessment from the measured data. Generally, two ways for compensating this motion are 1. the mechanical method by placing on top of a motion stabilizing platform (gimbal) which require additional hardware or 2. software-based motion correction algorithm mitigates the distortion incorporating motion input from IMU (inertial measuring unit) (Achtert et al., 2015; Tiana Alsina et al., 2015). Integrating an inertial measurement unit with the LiDAR can enable continuous autonomous long-term high-resolution shipborne measurements in different sea states.

8.3. Electrical safety

A ship is considered potentially a hazardous environment due to the presence of fuel, oxygen and ignition source, which may lead to fire and explosion. Therefore, while designing any electrical system for onboard use, it is a crucial factor which needs to be considered as it may provide a source of ignition. Either the equipment is required to have an intrinsic design or deployed away from the proximity of any hazard in accordance with SOLAS Ch II-1, Part D (IMO, 2014). The equipment needs to satisfy IECex directives that are accepted globally, or ATEX is accepted in EU, prior being installed in potentially explosive atmospheres such as on ships or offshore installations.

8.4. Weather protection

LiDAR equipment needs to provide high-quality measurement in order to fulfil the purpose of analysing sea spray accurately. The harsh marine climate can possess a significant challenge for such a study, especially if deployed for a longer time. Apart from waterproofing the LiDAR housing and corrosion protection, should have the arrangement to keep the optical module clean or installed in a location where the module is not obscured by saline water, dust or ice. Commercial LiDARs are generally designed to handle harsh climates of low temperature and devised inside a dustproof and waterproof casing. The ALS 300, Leosphere (2009), which was used for pesticide spray study (Gregorio et al., 2014), the optical head has a waterproof and dustproof rating of IP 65 and operating temperature range of $-15\,^\circ$C to $+35\,^\circ$C. The control unit can either be shielded in a casing or stored in a protected location such as inside the ship's bridge.

9. Conclusion

Marine icing is a very complicated phenomenon and involves many uncertainties, even with the present technological advancements and attempt of many researchers we do not have all the answers. However, from the reviews of past studies carried out in agricultural domain shows LiDAR has the potential to answer some important questions in the marine icing phenomenon by providing an approach to analyse the sea spray flux from a comprehensive perspective.

- LiDAR technology can provide spray cloud time-resolved information, thus has the ability to quantify droplet concentration in an entire sea spray cloud and total incoming water flux.
- Surface 2-D or volume 3-D range-resolved imaging of the sea spray cloud be possible with its scanning ability, whereas past methods used to study sea spray only could display data from specific parts of a spray cloud.
- This technique is also suitable for carrying out observations to validate present theoretical and analytical models (e.g. CFD) of sea spray propagation.
- A shipborne LiDAR suited for analysing incoming sea spray is possible to set up for carrying out autonomous measurements, thus can be deployed in multiple vessels, increasing the number of observations and data collection. Field measurements with the LiDAR system will allow us to produce more realistic data under several different conditions.

This review study proposes the use of LiDAR in the field of marine icing; however, further research and work remain to be done to recognize the full potential of the proposed method. In addition, short-range measurement can open the possibility to carry out other studies such as measurement of spray generated from wave impact in different parts of the ship other than bow like during beam winds and waves, the contribution of flux from ship's propeller wash, the variation of spray flux during synoptic-scale weather phenomena, the contribution of atmospheric icing and also can be utilized in the offshore and coastal facilities.

Declaration of competing interest

The authors declare no conflict of interest.

References

Achtert, P., Brooks, I.M., Brooks, B.J., Moat, B.I., Prytherch, J., Persson, P.O.G., Tjernström, M., 2015. Measurement of wind profiles by motion-stabilised ship-borne Doppler lidar. Atmos. Meas. Tech. 8 (11), 4993–5007. https://doi.org/10.5194/amt-8-4993-2015.

Aksyutin, L.R., 1979. Icing of Ships(in _Russian). Sudostroeyne Publishing House, Leningrad, p. 126.

Allard, M., Cayer, F., Champagne, Y., Babin, F., Cantin, D., 2007. Novel applications of an affordable short-range digital lidar. In: Lidar Remote Sensing for Environmental Monitoring VIII. Presented at the Optical Engineering + Applications, 2007. International Society for Optics and Photonics, San Diego, California, US, p. 66810L. https://doi.org/10.1117/12.733883.

Ansmann, A., Mattis, I., Wandinger, U., Wagner, F., Reichardt, J., Deshler, T., 1997. Evolution of the Pinatubo aerosol: Raman Lidar observations of particle optical depth, effective radius, mass and surface area over Central Europe at 53.4°N. J. Atmos. Sci. 54, 2630–2641. https://doi.org/10.1175/1520-0469(1997) 054<2630:EOTPAR>2.0.CO;2.

Bøckmann, A., Shipilova, O., Ekeberg, O.-C., 2019. Model assumptions in rig icing and their implications. In: Proceedings of the International Conference on Port and Ocean Engineering under Arctic Conditions. Presented at the 25th International Conference on Port and Ocean Engineering under Arctic Conditions (POAC 2019), Delft, Netherlands.

Bodaghkhani, A., Dehghani, S.R., Muzychka, Y.S., Colbourne, B., 2016. Understanding spray cloud formation by wave impact on marine objects. Cold Reg. Sci. Technol. 129, 114–136.

Borisenkov, Y.P., Panov, V.V., 1972. Basic results and prospects of research on hydrometeorological conditions of shipboard icing. Issledovaniye fizicheskoy prirody obledeneniya sudov (Leningrad). Cold Region. Res. Eng. Lab. 1–30. Draft Translation TL411, 1974.

Borisenkov, Y.P., Zablockiy, G.A., Makshtas, A.P., Migulin, A.I., Panov, V.V., 1975. On the approximation of the spray cloud dimensions (in Russian). In: Arkticheskii I Antarkticheskii Nauchno-Issledovatelskii Institut. Gidrometeoizdat Leningrad, pp. 121–126.

Brown, R.D., Roebber, P., 1985. The ice accretion problem in Canadian waters related to offshore energy and transportation. In: Candian Climate Centre, Atmospheric Environment Service. Rep 85-13, p. 295.

Cammaert, G., 2013. Impact of marine icing on Arctic offshore operations. In: Arctic Marine Operations Challenges & Recommendations, vol. 5 (Pilot Project).

Cantin, D., Babin, F., Levesque, M., 2007. Real-time Measuring of the Spatial Distribution of Sprayed Aerosol Particles. United States Patent No. US20070076202A1. https://patents.google.com/patent/US20070076202A1/en.

Chung, V.K.K., 1995. Ship Icing and Stability. Doctoral thesis. University of Alberta, Canada.

Collis, R.T.H., 1968. Lidar observations of atmospheric motion in forest valleys. Bull. Am. Meteorol. Soc. 49, 918–923. https://doi.org/10.1175/1520-0477.49.9.918.

Collis, R.T.H., Russell, P.B., 1976. Lidar measurement of particles and gases by elastic backscattering and differential absorption. In: Hinkley, E.D. (Ed.), Laser Monitoring of the Atmosphere, E. D. Hinkley. Springer, Berlin/Heidelberg, pp. 71–151. https://doi.org/10.1007/3-540-07743-X_18.

Comiskey, A.L., Leslie, L.D., Wise, J.L., 1984. Superstructure Icing and Forecasting in Alaskan Waters. University of Alaska Arctic Environmental Information and Data Center, p. 30 (Unpublished).

DeAngelis, R.M., 1974. Superstructure icing. Mar. weather Log. 18 (1), 1–7.

Dehghani, S.R., Muzychka, Y.S., Naterer, G.F., 2016a. Droplet trajectories of wave-impact sea spray on a marine vessel. Cold Reg. Sci. Technol. 127, 1–9. https://doi.org/10.1016/j.coldregions.2016.03.010.

Dehghani, S.R., Naterer, G.F., Muzychka, Y.S., 2016b. Droplet size and velocity distributions of wave-impact sea spray over a marine vessel. Cold Reg. Sci. Technol. 132, 60–67. https://doi.org/10.1016/j.coldregions.2016.09.013.

Dehghani-Sanij, A.R., Muzychka, Y.S., Naterer, G.F., 2015. Analysis of ice accretion onVertical surfaces of marine vessels and structures in arctic conditions. In: Proceedings of the ASME 2015 34th International Conference on Ocean, Offshoreand Arctic Engineering May 31–June 5, 2015 Newfoundland,Canada. ASME, OMAE2015-41306, p. 7. https://doi.org/10.1115/OMAE2015-41306.

Dehghani-Sanij, A.R., Dehghani, S.R., Naterer, G.F., Muzychka, Y.S., 2017a. Sea spray icing phenomena on marine vessels and offshore structures: review and formulation. Ocean Eng. 132, 25–39. https://doi.org/10.1016/j.oceaneng.2017.01.016.

Dehghani-Sanij, A.R., Dehghani, S.R., Naterer, G.F., Muzychka, Y.S., 2017b. Marine icing phenomena on vessels and offshore structures: prediction and analysis. Ocean Eng. 143, 1–23. https://doi.org/10.1016/j.oceaneng.2017.07.049.

DNVGL, 2019. DNVGL-OS-A201 Edition July 2019 Winterization for Cold Climate Operations. Rules and Standard. Copyright © DNV GL. Retrieved from. https://rules.dnvgl.com/docs/pdf/DNVGL/OS/2019-07/DNVGL-OS-A201.pdf.

Edner, H., Ragnarson, P., Wallinder, E., 1995. Industrial emission control using lidar techniques. Environ. Sci. Technol. 29, 330–337.

Fiocco, G., Smullin, L.D., 1963. Detection of scattering layers in the upper atmosphere (60–140 km) by optical radar. Nature 199, 1275–1276. https://doi.org/10.1038/1991275a0.

Forest, T.W., Lozowski, E.P., Gagnon, R., 2005. Estimating marine icing on offshore structures using RIGICE04. In: Proceedings of the 11th International Workshop on Atmospheric Icing on Structures (IWAIS) 12-16 Jun 2005, Montreal, Quebec, Canada, pp. 45–52.

Fuentes, E., Coe, H., Green, D., de Leeuw, G., McFiggans, G., 2010. Laboratory-generated primary marine aerosol via bubble bursting and atomization. Atmos. Meas. Tech. 3, 141–162.

Fukuchi, T., Shiina, T., 2012. Industrial Applications of Laser Remote Sensing. Bentham Science Publishers, p. 194.

Gregorio, E., Rosell-Polo, J.R., Sanz, R., Rocadenbosch, F., Solanelles, F., Garcerá, C., Chueca, P., Arnó, J., del Moral, I., Masip, J., Camp, F., Viana, R., Escolà, A., Gràcia, F., Planas, S., Moltó, E., 2014. LIDAR as an alternative to passive collectors to measure pesticide spray drift. Atmos. Environ. 82, 83–93. https://doi.org/10.1016/j.atmosenv.2013.09.028.

Gregorio, E., Rocadenbosch, F., Sanz, R., Rosell-Polo, J.R., 2015. Eye-safe lidar system for pesticide spray drift measurement. Sensors 15, 3650–3670. https://doi.org/10.3390/s150203650.

Gregorio, E., Torrent, X., Planas de Martí, S., Solanelles, F., Sanz, R., Rocadenbosch, F., Masip, J., Ribes-Dasi, M., Rosell-Polo, J.R., 2016a. Measurement of spray drift with a specifically designed lidar system. Sensors 16, 499. https://doi.org/10.3390/s16040499.

Gregorio, E., Torrent, X., Solanelles, F., Sanz, R., Rocadenbosch Burillo, F., Masip, J., Ribes Dasi, M., Planas, S., Rosell Polo, J.R., 2016b. Lidar: towards a new methodology for field measurement of spray drift. Asp. Biol. 201–206.

Gregorio López, E., 2012. Lidar Remote Sensing of Pesticide Spray Drift. Ph.D. Thesis. Universitat de Lleida, Spain, p. 126.

Guest, P., Luke, R., 2005. Vessel icing. Mar. weather Log. 49, 9.

Hansen, E.S., 2012. Numerical Modelling of Marine Icing on Offshore Structures and Vessels. Master's thesis. NTNU - Norwegian University of Science and Technology.

Hay, R.F.M., 1956. Meteorological aspects of the loss of Lorella and Roderigo. Mar. Observ. 26, 89–94.

Hiscox, A.L., Miller, D.R., Nappo, C.J., Ross, J., 2006. Dispersion of fine spray from aerial applications in stable Atmospheric conditions. Trans. ASABE St Joseph Mich. 49 (5), 1513–1520. https://doi.org/10.13031/2013.22043.

Hoff, R.M., Mickle, R.E., Froude, F.A., 1989. A rapid acquisition lidar system for aerial spray diagnostics. Trans. ASAE 32, 1523–1528. https://doi.org/10.13031/2013.31183.

Horjen, I., 1990. Numerical Modeling of Time-dependent Marine Icing, Anti-icing and De-icing. Ph.D. Thesis. Trondheim Univ., Norway, p. 159.

Horjen, I., 2015. Offshore drilling rig ice accretion modeling including a surficial brine film. Cold Reg. Sci. Technol. 119, 84–110. https://doi.org/10.1016/j.coldregions.2015.07.006.

Horjen, I., Vefsnmo, S., 1984. Mobile Platform Stability (MOPS) Subproject 02 – Icing, vol. 283021. Norwegian Hydrodynamic Laboratories, River and Harbour Laboratory, p. 121.

Horjen, I., Loeset, S., Vefsnmo, S., 1986. ICING HAZARDS ON SUPPLY VESSELS AND STAND-BY BOATS (No. STF60 A 86073). Norwegian Hydrotechnical Laboratory, Norway, Trondheim.

Hulburt, E.O., 1937. Observations of a searchlight beam to an altitude of 28 kilometers. J. Opt. Soc. Am. 27, 377–382. https://doi.org/10.1364/JOSA.27.000377.

IMO, 2014. International Convention for Safety of Life at Sea, 2014 edition. International Maritime Organization, London.

IMO, 2016. International Code of Safety for Ships Operating in Polar Waters (Polar Code), 2016 edition. International Maritime Organization, London.

IMO, 2020. International Code on Intact Stability, 2020 edition. International Maritime Organization, London. 2008.

Itagaki, K., 1977. Icing on ships and stationary structures under marine conditions. A preliminary literature survey of Japanese sources. Special Report SR 77-27. US Army Cold Regions Research and Engineering Laboratory, Hanover, NH.

Itagaki, K. 1984. Icing rate on stationary structures under marine conditions. CRREL Report 84-12. Hanover, NH: US Army Cold Regions Research and Engineering Laboratory.

Johansen, J., Edvardsen, K., Sharma, P., Khawaja, H., 2015. Measuring the sea spray flux using high-speed camera. In: Poster Presentation at the International Conference of Multiphysics, December 2015. London, United Kingdom. https://doi.org/10.13140/RG.2.2.34044.74884.

Jones, K.F., Andreas, E.L., 2013. Winter measurements of sea spray at Mt. Desert Rock. In: Proceedings of the 16th International Workshop on the Atmospheric Icing of Structures, St. John's Newfoundland, September 2013.

Jørgensen, T.S., Vefsnmo, S., Horjen, I., 1986. Offshore Icing – Phase II Final Report (No. STF60 F 86084). Norwegian Hydrotechnical Laboratory, Norway, Trondheim.

Kachurin, L., Gashin, L., Smirnov, I., 1974. Icing rate of small displacement fishing vessels under various hydrometeorological conditions. Meteorol. Gidrol. 3, 50–60.

Kato, R., 2012. Modelling of Ship Superstructure Icing. Master Thesis. Norwegian University of Science and Technology, Trondheim, Norway.

Khot, L., Miller, D., Hiscox, A., Salyani, M., Walker, T., Farooq, M., 2011. Extrapolation of droplet catch measurements in aerosol application treatments. At. Sprays 21, 149–158. https://doi.org/10.1615/AtomizSpr.2011002846.

Kong, Z., Liu, Z., Zhang, L., Guan, P., Li, L., Mei, L., 2018. Atmospheric pollution monitoring in urban area by employing a 450-nm lidar system. Sensors 18, 1880. https://doi.org/10.3390/s18061880.

Koyama, M., Shiina, T., 2011. Development of LED mini-lidar. In: 2011 International Quantum Electronics Conference (IQEC) and Conference on Lasers and Electro-Optics (CLEO) Pacific Rim Incorporating the Australasian Conference on Optics, Lasers and Spectroscopy and the Australian Conference on Optical Fibre Technology 28 Aug - 1 Sep,2011. IEEE, Sydney, NSW, Australia, pp. 544–545. https://doi.org/10.1109/IQEC-CLEO.2011.6193859.

Kulyakhtin, A., Tsarau, A., 2014. A time-dependent model of marine icing with application of computational fluid dynamics. Cold Reg. Sci. Technol. 104–105, 33–44. https://doi.org/10.1016/j.coldregions.2014.05.001.

Kuzniecov, V.P., Kultashev, Y.N., Panov, V.V., Tiurin, A.P., Sharapov, A.V., 1971. Field investigations of ship icing in the Japan Sea in 1969. In: Theoretical and Experimental Investigations of the Conditions of the Icing. Gidrometeoizdat Leningrad, pp. 57–69.

Leosphere, 2009. Cloud & Aerosol Lidar for Atmospheric Monitoring (ALS 300/450 Product Information. Orsay, France).

Lolli, Simone, Sauvage, L., Loaec, S., Lardier, M., 2011. EZ Lidar™: a new compact autonomous eye-safe scanning aerosol Lidar for extinction measurements and PBL

height detection. Validation of the performances against other instruments and intercomparison campaigns. Óptica Pura Apl. 44, 33–41.

Lozowski, E.P., Szilder, K., Makkonen, L., 2000. Computer simulation of marine ice accretion. Philos. Trans. R. Soc. Math. Phys. Eng. Sci. 358, 2811–2845. https://doi.org/10.1098/rsta.2000.0687.

Lundquist, J.E., Udin, I., 1977. Ice accretion on ships with special emphasis on Baltic conditions, 23. Winter Navigation Research Board, p. 34.

Madonna, F., Amato, F., Vande Hey, J., Pappalardo, G., 2014. Ceilometer aerosol profiling vs. Raman lidar in the frame of INTERACT campaign of ACTRIS. Atmos. Meas. Tech. Disc. 7, 12407–12447. https://doi.org/10.5194/amtd-7-12407-2014.

Makkonen, L., 1984. Atmospheric Icing on Sea Structures. U.S. Army Cold Regions Researchand Engineering Laboratory: CRREL Monograph, 84-2.

Makkonen, L., 1987. Salinity and growth rate of ice formed by sea spray. Cold Reg. Sci. Technol. 14, 163–171. https://doi.org/10.1016/0165-232X(87)90032-2.

Makkonen, L., 2000. Models for the growth of rime, glaze, icicles and wet snow on structures. Philos. Trans. R. Soc. Math. Phys. Eng. Sci. 358, 2913–2939. https://doi.org/10.1098/rsta.2000.0690.

McManamon, P.F., 2019. Significant applications of LiDAR Ch-11. In: LiDAR Technologies and Systems. SPIE. https://doi.org/10.1117/3.2518254.ch11.

Measures, R., 1992. Laser Remote Sensing: Fundamentals and Applications. Krieger Publishing Company, Malabar, FL.

Mertins, H.O., 1968. Icing of fishing vessels due to spray. Mar. Obs. 38 (221), 128–130.

Mickle, R.E., 1994. Utilizing vortex behaviour to minimize drift. J. Environ. Sci. Health., B 29, 621–645. https://doi.org/10.1080/03601239409372897.

Mickle, R.E., 1996. Influence of aircraft vortices on spray cloud behaviour. J. Am. Mosq. Contr. Assoc. 12 (2), 372–379.

Mickle, R.E., 1999. Analysis of Lidar Studies Conducted during Aerial Spray Drift Trials. REMPSpC Report, Ayr, Ontario, Canada.

Miller, D., Stoughton, T., 2000. Response of spray drift from aerial applications at forest edge to atmospheric stability. Agric. For. Meteorol. 100, 49–58. https://doi.org/10.1016/S0168-1923(99)00084-2.

Miller, D., Salyani, M., Hiscox, A., 2003. Remote measurement of spray drift from orchard sprayer using LIDAR. In: Proceedings of the 2003 ASAE Annual Meeting. American Society of Agricultural and Biological Engineers. Paper No. 031093.

Miller, D.R., Khot, L.R., Hiscox, A.L., Salyani, M., Walker, T.W., Farooq, M., 2012. Effect of atmospheric conditions on coverage of fogger applications in a desert surface boundary layer. Trans. ASABE (Am. Soc. Agric. Biol. Eng.) 55, 351–361. https://doi.org/10.13031/2013.41373.

Mintu, S., Molyneux, D., Oldford, D., 2016. State-of-the-art review of research on ice accretion measurements and modelling. In: Arctic Technology Conference. Offshore Technology Conference,24-26 October.St. John's, Newfoundland and Labrador, Canada.OTC. https://doi.org/10.4043/27422-MS.

Miya, H., Shiina, T., Kato, T., Noguchi, K., Fukuchi, T., Asahi, I., Sugimoto, S., Ninomiya, H., Shimamoto, Y., 2009. Compact Raman lidar for hydrogen gas leak detection. In: Conference on Lasers and Electro-Optics/Pacific Rim 30 August–3 September 2009. Optical Society of America, Shanghai China, p. ME1_3.

Muenkel, C., Emeis, S., Mueller, W.J., Schaefer, K.P., 2004. Aerosol concentration measurements with a lidar ceilometer: results of a one year measuring campaign. In: Remote Sensing of Clouds and the Atmosphere VIII. International Society for Optics and Photonics, pp. 486–496.

Muzik, I., Kirby, A., 1992. Spray overtopping rates for Tarsiut Island: model and field study results. Can. J. Civ. Eng. 19 https://doi.org/10.1139/l92-057.

NTSB, 2018. Capsizing and Sinking of Fishing Vessel Destination Due to Heavy Freezing Spray Conditions. National Transportation Safety Board. February 11, 2017 Accident Report, DCA17FM006. Retrieved rom. https://www.ntsb.gov/investigations/Accide ntReports/Reports/MAB1814.pdf.

Ong, P., Shiina, T., Manago, N., Kuze, H., Senshu, H., Otobe, N., Hashimoto, G., Kawabata, Y., 2018. A compact led lidar system fitted for a mars rover - design and ground experiment. EPJ Web Conf. 176, 02013, 2018.

Ono, N., 1964. Studies on the Ice Accumulation on Ships. 2. On the Conditions for the Formation of Ice and the Rate of Icing. Low Temperature Sci, pp. 171–181. A22 (in Japanese with English summary).

Orimolade, A.P., Gudmestad, O.T., Wold, L.E., 2017. Vessel stability in polar low situations. Ships Offshore Struct. 12, S82–S87. https://doi.org/10.1080/17445302.2016.1259954.

Overland, J.E., 1990. Prediction of vessel icing for near-freezing sea temperatures. Weather Forecast. 5, 62–77. https://doi.org/10.1175/1520-0434(1990)005<0062: POVIFN>2.0.CO;2.

Overland, J.E., Pease, C.H., Preisendorfer, R.W., Comiskey, A.L., 1986. Prediction of vessel icing. J. Clim. Appl. Meteorol. 25 (12), 1793–1806. https://doi.org/10.1175/1520-0450(1986)025<1793:POVI>2.0.CO;2.

Ozeki, T., Sagawa, G., 2013. Field observation of seawater spray droplets impinging on the upper deck of an icebreaker. In: Proceedings of the International Conference on Port and Ocean Engineering under Arctic Conditions. Port and Ocean Engineering under Arctic Conditions (POAC)2013-6-9 to 2013-6-13.Espoo, Finland, p. 7.

Ozeki, T., Shiga, T., Sawamura, J., Yashiro, Y., Adachi, S., Yamaguchi, H., 2016. Development of sea spray meters and an analysis of sea spray characteristics in large vessels. In: Presented at the the 26th International Ocean and Polar Engineering Conference. International Society of Offshore and Polar Engineers 26 June-2 July, Rhodes, Greece, p. 1335.

PAME, 2020. The Increase in Arctic Shipping 2013-2019. Arctic Ship Status Report (ASSR) Project, PAME - Arctic Shipping Status Report #1. The Protection of the Arctic Marine Environment. © 2020 PAME. Retrieved From. https://www.pame.is /document-library/shipping-documents/arctic-ship-traffic-data-documents/reports /arctic-shipping-status-reports-jpg-version/arctic-shipping-report-1-the-inc rease-in-arctic-shipping-2013-2019-jpgs.

Panov, V.V., 1976. Icing of Ships. Arkticheskii I Antarkti- Cheskii Nauchno-Issledovatelskii Institut. In: Trudy 334. Gidrometeoizdat, Leningrad, p. 263 (in Russian).

Rashid, T., Khawaja, H.A., Edvardsen, K., 2016. Review of marine icing and anti-/de-icing systems. J. Mar. Eng. Technol. 15 (2), 79–87. https://doi.org/10.1080/20464177.2016.1216734.

Richardson, B., Strand, T., Thistle, H.W., Hiscox, A., Kimberley, M.O., Schou, W.C., 2017. Influence of a young pinus radiata canopy on aerial spray drift. Trans. ASABE (Am. Soc. Agric. Biol. Eng.) 60 (6), 1851–1861. https://doi.org/10.13031/trans.12497.

Roebber, P., Mitten, P., Canadian Climate Centre., & Canada, 1987. Modelling and measurement of icing in Canadian waters. Report number: 87-15. Atmospheric Environment Service, Downsview, Ont. https://www.worldcat.org/title/modelling-a nd-measurement-of-icing-in-canadian-waters/oclc/456567088.

Ryerson, C.C., 1995. Superstructure spray and ice accretion on a large U.S. Coast Guard cutter. Atmospheric Res., Atmospheric icings of structures 36, 321–337. https://doi.org/10.1016/0169-8095(94)00045-F.

Ryerson, C.C., 2013. Icing Management for Coast Guard Assets. Cold Regions Research and Engineering Laboratory, US Army Engineer Research and Development Centre, Hanover (NH), p. 529. ERDC/CRREL TR-13-7.

Saha, D., Dehghani, S.R., Pope, K., Muzychka, Y., 2016. Temperature distribution during solidification of saline and fresh water droplets after striking a super-Cooled surface. In: Presented at the Arctic Technology Conference, 24-26 October, St. John's, Newfoundland and Labrador, Canada. https://doi.org/10.4043/27421-MS.

Samuelsen, E.M., Graversen, R.G., 2019. Weather situation during observed ship-icing events off the coast of Northern Norway and the Svalbard archipelago. Weather Clim. Extrem. 24, 100200. https://doi.org/10.1016/j.wace.2019.100200.

Samuelsen, E.M., Løset, S., Edvardsen, K., 2015. Marine icing observed on KV Nordkapp during a cold air outbreak with a developing polar low in the Barents Sea. In: Proceedings of the 23rd International Conference on Port and Ocean Engineering under Arctic Conditions; 2015 Jun 14–18; Trondheim, Norway.

Samuelsen, E.M., Edvardsen, K., Graversen, R.G., 2017. Modelled and observed sea-spray icing in Arctic–Norwegian waters. Cold Reg. Sci. Technol. 134, 54–81. https://doi.org/10.1016/j.coldregions.2016.11.002.

Sassen, K., 1975. Laser depolarisation 'bright band' from melting snowflakes. Nature 255, 316–318. https://doi.org/10.1038/255316a0.

Sawada, T., 1962. Icing on Ships and the Forecasting Method. (In Japanese). Snow and Ice, pp. 12–14, 24.

Sharapov, A.V., 1971. On the intensity of superstructure icing of small vessels (MFV type). Theoretical and experimental investigations of the conditions of ship icing. Gidrometeoizdat Leningr 95–97.

Shekhtman, A.N., 1968. The probability and intensity of the icing-up of ocean-going vessels. In: Moskow Nauk-Issled Inst. Aeroklim, T. Vyp 50, pp. 55–65.

Shellard, H.C., 1974. The Meteorological Aspects of Ice Accretion on Ships. Marine Science Affairs Report Technical Report 10. World Meteorological Organization, Geneva, Switzerland.

Shiina, T., 2010. Optical design for near range lidar. In: Proc. SPIE 7860, Lidar Remote Sensing for Environmental Monitoring XI, 78600B. Presented at the SPIE Asia-Pacific Remote Sensing 11 Nov 2010, SPIE, Incheon, S. Korea. https://doi.org/10.1117/12.869568.

Shiina, T., 2013. LED mini-lidar for air and dust monitoring. In: Proc. SPIE 8905, International Symposium on Photoelectronic Detection and Imaging 19 Sep 2013. Laser Sensing and Imaging and Applications. SPIE, Beijing, China, p. 890533. https://doi.org/10.1117/12.2042370.

Shiina, T., 2019a. LED mini lidar for atmospheric application. Sensors 19, 569. https://doi.org/10.3390/s19030569.

Shiina, T., 2019b. Sea wave dynamics visualization and its interaction with the surface atmosphere by LED mini-lidar. In: Presented at the Proc. SPIE 11150, Remote Sensing of the Ocean, Sea Ice, Coastal Waters, and Large Water Regions 14th Oct 2019. SPIE, Strasbourg, France. https://doi.org/10.1117/12.2533406.

Shiina, Tatsuo, 2020. Atmosphere activity measurement by LED Raman mini lidar. EPJ Web Conf. 237, 07002 https://doi.org/10.1051/epjconf/202023707002.

Shiina, T., Koyama, M., 2010. M. LED Lidar System. Japanese Patent Application No. 2010-275798, 10 October 2010.

Shiina, T., Noguchi, K., Tsuji, K., 2015. Compact and mini Raman lidars for hydrogen gas detection. In: Presented at the Proceedings of the 23th International Conference on Nuclear Engineering (ICONE-23), Chiba, Japan, p. 3737.

Shiina, T., Yamada, S., Senshu, H., Otobe, N., Hashimoto, G., Kawabata, Y., 2016. LED minilidar for Mars rover. In: Proc. SPIE 10006, Lidar Technologies, Techniques, and Measurements for Atmospheric Remote Sensing XII, 100060F. Presented at the SPIE Remote Sensing 24 Oct 2016. SPIE, Edinburgh, United Kingdom. https://doi.org/10.1117/12.2241976.

Shipilova, O., Kulyakhtin, A., Tsarau, A., Libby, B., Moslet, P.O., Loset, S., 2012. Mechanism and dynamics of marine ice accretion on vessel archetypes. In: Offshore Technology Conference OTC-23762-MS; 3-5 December.Houston, TX, United States. https://doi.org/10.4043/23762-MS.

Song, X., Zhai, X., Liu, L., Wu, S., 2017. Lidar and ceilometer observations and comparisons of atmospheric cloud structure at Nagqu of Tibetan Plateau in 2014 summer. Atmosphere 8, 9. https://doi.org/10.3390/atmos8010009.

Song, Z., Zhang, B., Feng, H., Zhu, S., Hu, L., Brydegaard, M., Li, Y., Jansson, S., Malmqvist, E., Svanberg, K., Zhao, G., Bood, J., Svanberg, S., Li, D., 2020. Application of lidar remote sensing of insects in agricultural entomology on the Chinese scene. J. Appl. Entomol. 144, 161–169. https://doi.org/10.1111/jen.12714.

Spinhirne, J.D., 1993. Micro-pulse lidar. IEEE Trans. Geosci. Rem. Sens. 31, 48–55. https://doi.org/10.1109/36.210443.

Spinhirne, J.D., 1994. Micro pulse lidar systems and applications. In: Proceedings of 17th International Laser Radar Conference 25–29 July 1994.Chiba, Japan, pp. 162–165.

Stallabrass, J.R., 1980. Trawler Icing - A Compilation of Work Done at the National Research Council. Mechanical Engineering Report MD-56. National Research Council Canada, Ottawa, Ontario, Canada.

Stoughton, T.E., Miller, D.R., Yang, X., Ducharme, K.M., 1997. A comparison of spray drift predictions to lidar data. Agric. For. Meteorol. 88, 15–26. https://doi.org/10.1016/S0168-1923(97)00056-7.

Sultana, K.R., Dehghani, S.R., Pope, K., Muzychka, Y.S., 2018. A review of numerical modelling techniques for marine icing applications. Cold Reg. Sci. Technol. 145, 40–51. https://doi.org/10.1016/j.coldregions.2017.08.007.

Tabata, T., 1969. Studies on the ice accumulation on ships III. Low Temp. Sci. Ser. Phys. Sci. 27, 339–349.

Tabata, T., Iwata, S., Ono, N., 1963. Studies on the ice accumulation on ships I. Low Temp. Sci. Ser. A 21, 173–221.

Teigen, S.H., Ekeberg, O.-C., Myhre, B., Rustad, H., Petersen, S., Schrøder-Bråtane, E., Carlsen, S., 2019. Autonomous real-time sea spray measurement system for offshore structures. In: Proc. 25th Int. Conf. Port Ocean Eng. Arct. Cond. June 9-13 2019 Delft Neth., vol. 10.

Tiana Alsina, J., Gutiérrez Antuñano, M.Á., Würth, I., Puigdefàbregas Sagristà, J., Rocadenbosch Burillo, F., 2015. Motion compensation study for a floating Doppler wind lidar. In: Presented at the 2015 IEEE International Geoscience & Remote Sensing Symposium: Proceedings: July 26–31, 2015. Institute of Electrical and Electronics Engineers (IEEE), Milan, Italy, pp. 5379–5382. https://doi.org/10.1109/IGARSS.2015.7327051.

Torrent, X., Gregorio, E., Rosell-Polo, J.R., Arnó, J., Peris, M., van de Zande, J.C., Planas, S., 2020. Determination of spray drift and buffer zones in 3D crops using the ISO standard and new LiDAR methodologies. Sci. Total Environ. 714, 136666. https://doi.org/10.1016/j.scitotenv.2020.136666.

Tsai, M.Y., 2007. The Washington Spray Drift Studies: Understanding the Broader Mechanisms of Pesticide Spray Drift (PhD Thesis). Ph. D Thesis, University of Washington, Seattle, WA, USA.

Wise, J.L., Comiskey, A.L., 1980. Superstructure Icing in Alaskan Waters. US Department of Commerce, National Oceanic and Atmospheric Administration, Environmental Res. Laboratories.

WMO, 1994. Guide to the Applications of Marine Climatology. Secretariat of the World Metrological Organization, Geneva.

Wold, L.E., 2014. A Study of the Changes in Freeboard, Stability and Motion Response of Ships and Semi-submersible Platforms Due to Vessel Icing (Master Thesis). University of Stavanger, Norway.

Zakrzewski, W.P., 1986. Icing of Ships, Part 1, Splashing a Ship with Spray. Technical Report NOAA Technical Memorandum ERL PMEL 66. National Oceanic and Atmospheric Administration. Seattle, Washington, USA.

Zakrzewski, W.P., 1987. Splashing a ship with collision-generated spray. Cold Reg. Sci. Technol. 14, 65–83.

Zakrzewski, W.P., Lozowski, E.P., Muggeridge, D., 1988. Estimating the extent of the spraying zone on a sea-going ship. Ocean Eng. 15, 413–429. https://doi.org/10.1016/0029-8018(88)90008-X.